JOURNAL OF CATALYSIS **161,** 20–30 (1996)
ARTICLE NO. 0158

Shape-Selective Methylamine Synthesis over Small-Pore Zeolite Catalysts

Martin C. Ilao,[1] Hiromichi Yamamoto,[2] and Kohichi Segawa[3]

Department of Chemistry, Faculty of Science and Technology, Sophia University, 7-1 Kioi-cho, Chiyoda-ku, Tokyo 102, Japan

Received July 13, 1995; revised December 6, 1995; accepted February 2, 1996

Methylamine syntheses from methanol and ammonia on various zeolite catalysts have been studied over a temperature range of 573–673 K. The H-chabazite catalyst gives enhanced yield of monomethylamine at higher partial pressures of ammonia, while the formation of trimethylamine and dimethyl ether has been extremely retarded. Sorption–desorption experiments reveal nearly complete exclusion of TMA from the chabazite cages. Sorption and IR spectroscopic data provide evidence that the initial methylamine formation involves methanol and ammonia that are both bound to Brønsted acid sites and follows a Langmuir–Hinshelwood mechanism, in contrast to the Eley–Rideal mechanism that is observed with large pore zeolites or other solid catalysts. Transition state selectivity, rather than product selectivity, is invoked as the main cause for the preponderance of monomethylamine and dimethylamine and the almost complete suppression of trimethylamine.

INTRODUCTION

Methylamines are important intermediates in the manufacture of nitrogen-containing products (1). Commercially, they are produced by amination of methanol (Eqs. [1]–[3]) over amorphous silica–alumina catalysts. At $NH_3/CH_3OH = 1.9$ and 623 K, a 99.8% methanol conversion gives an equilibrium distribution of monomethylamine (MMA), dimethylamine (DMA), and trimethylamine (TMA) of 15.1, 22.8, and 62.1 wt%, respectively (2). In recent years, a considerable research effort has been devoted to find catalysts with superior activity and high selectivity for MMA and DMA, but low selectivity for TMA (3–9). Such a catalyst can suppress TMA; this is desirable because TMA forms complex azeotropic mixtures with ammonia, MMA, and DMA; in such cases, product separation becomes complicated and costly (9):

	K (673 K)	
$CH_3OH + NH_3 \rightleftharpoons CH_3NH_2 + H_2O$	41.8	[1]
$CH_3OH + CH_3NH_2 \rightleftharpoons (CH_3)_2NH + H_2O$	187	[2]
$CH_3OH + (CH_3)_2NH \rightleftharpoons (CH_3)_3N + H_2O$	324.	[3]

Conventional amorphous acidic oxide catalysts that are now in commercial use are incapable of giving DMA selectivities beyond the thermodynamic values. Below 573 K, catalyst activity is low, while above 723 K the yield of unwanted products increases; these include carbon dioxide, methane, ethane, and formaldehyde (3). At N/C ratios below 0.67, catalyst deactivation is rapid, while the good selectivities obtainable at high N/C ratios are offset by the large apparatus required for large volumes of ammonia to be recirculated. Amination reactions typically are conducted between 573 and 723 K, at 1.5–3 MPa (9, 10), and with N/C ratios between 0.67 and 5.

Several approaches to altering the equilibrium product ratio involve use of solid catalysts with variations in acid strength, in type of acid centers, and in zeolite pore geometry.

The use of γ-Al_2O_3 as catalyst (573–673 K) gave mainly DME and only traces of alkylamines, thereby ruling out a purely Lewis acid-catalyzed mechanism. Mochida *et al.* (11) predicted an increase in MMA and DMA selectivities upon decreasing the catalyst acid strength. Weigert also proposed that Na-mordenite catalysts would show lower selectivity for TMA (3). However, the catalytic activity over Na-mordenite is lower than that of H-mordenite. Dingerdissen obtained only very small amounts of alkylamines from methanol amination between 573 and 673 K over alkaline forms of MFI (ZSM-5), KFI (ZK-5), and LEV (LZ-132) catalysts (12). The Na-form of zeolites can catalyze methylamine formation with good selectivities, although the activity is low. The reaction involves bound methanol (more strongly on Na than on H) with free ammonia to give the alkylamines. If the catalyst is Brønsted acid, ammonia

[1] Current address: Department of Chemistry, De La Salle University, Manila, Philippines.

[2] Current address: Tokyo Gas Co., Ltd., Fundamental Technology Research Laboratory, 1-16-25 Shibaura, Minato-ku, Tokyo 105, Japan.

[3] To whom correspondence should be addressed.

0021-9517/96 $18.00

is bound more strongly than methanol; alkylamines are formed by the reaction between bound ammonia and free methanol (13).

Fetting and Dingerdissen have shown that selectivity depends less on acid strength than on the shape discrimination of the catalyst (14). Zeolite shape-selectivity can take place only inside the pore system. However, although the outer surface of a zeolite accounts for less than 5% of its total surface, nonselective outer-surface reactions may not be negligible. To make use of the shape selectivity of a zeolite, one must eliminate the external catalytic sites. Even so, zeolite pore orifices may be considerably larger than those determined by XRD due to framework vibrations under catalytic conditions (573–673 K). Higher reaction temperatures can vitiate selectivities at lower temperatures. Shannon and co-workers found that small pore zeolites RHO (H-RHO), KFI (H-ZK-5), and CHA (chabazites) are not only significantly more active but exhibit selectivities much greater than those previously reported for other zeolites (4, 7, 8, 15, 16). Corbin and co-workers studied the relative contributions of internal and external acid sites of small pore H-RHO zeolites; and upon vapor phase trimethylphosphite treatment of the external sites, TMA formation was essentially suppressed (17). Niiyama and co-workers used a desorption control mechanism to completely suppress TMA formation in methylamine synthesis over a heteropolyacids catalyst above 750 K (18).

Recently, we reported that modified mordenite catalysts previously treated with $SiCl_4$ and ion-exchanged from Na-form to H-form showed excellent selectivity (99%, MMA plus DMA) at about 90% methanol conversion ($NH_3/CH_3OH = 1.0$, 633 K) (19). Such selectivity was achieved by narrowing the mordenite pore aperture close to the kinetic diameter of DMA (0.44 nm) (20). This result implies that product selectivity, rather than transition state selectivity, governs amination selectivity; the intrinsic pore size of the mordenite framework itself does not provide control of shape selectivity.

In this work, we report methanol aminations over zeolites, particularly the chabazites, which have smaller pore openings than mordenites (0.38 vs 0.65 nm pore size). We also employed sorption experiments and infrared spectroscopy of adsorbed species to probe the mechanism of amination reaction on these catalysts. Sorption and infrared data suggest that the initial amination step in mordenite is different from chabazite. The Eley–Rideal mechanism operates in mordenites: the basic (ammonia and amines) component is adsorbed at the Brønsted acid center and the alcohol reacts from the gas phase with adsorbed base (14), while the Langmuir–Hinshelwood mechanism is involved in chabazites. In chabazites, the reactive ammonia and methanol species are both bound to catalytic sites. Since chabazite cages are too narrow to permit reaction between bound species and another free molecule, we ascribe the high selectivity herein obtained to "transition-state selectivity" rather than to "product selectivity." The same transition-state selectivity may be responsible for the fact that the chabazite catalyst underwent no deactivation throughout the reactions: bulky molecules from adsorbed and gaseous reactants were precluded from forming and being trapped, which would have resulted in coke formation and eventually catalyst deactivation.

EXPERIMENTAL

Preparation of catalysts. Zeolites (JRC-Z), silica–alumina (JRC-SAL-2, Si/Al = 5.3), and alumina (JRC-ALO-2) samples were supplied by the Catalysis Society of Japan (JRC, Japan Reference Catalysts). Three different types of zeolites were studied: H-FAU (H-Faujasite-Y: JRC-Z-HY5.6, Si/Al = 5.3), H-MOR (H-mordenite: JRC-HM20, Si/Al = 9.7), and H-MFI (H-ZSM-5: JRC-Z5-25H, Si/Al = 12.5). The smaller pore size zeolites, K-FER (K-ferrierite: TSZ-720KOA, Si/Al = 8.4) and K-CHA (K-chabazite, Si/Al = 2.4), were supplied by TOSOH and by Air Products and Chemicals, Inc., respectively. Samples of zeolites in Na-form or K-form were ion-exchanged to H-form with an aqueous solution of NH_4NO_3. They were dried at 373 K for 24 h, calcined in the furnace at a constant temperature increase (2 K min^{-1}) from 373 to 773 K, and finally kept at 773 K for 5 h.

Catalytic reactions. Methylamine syntheses were carried out at 573–653 K in a flowing reaction system at atmospheric pressures with a mixture of NH_3, CH_3OH, and N_2 at a flow rate of 54 cm^3 min^{-1}. Before the reaction, the catalyst (250–1000 mg) was calcined at 773 K under O_2 flow for 2 h. The products were analyzed by a gas chromatograph (TCD) which was equipped with a 4.6-m × 3.2-mm i.d. column of PEG-400 (25%) + KOH (2.5%) on acid-washed Chromosorb W at 358 K (2). The methanol conversion and selectivities were calculated in carbon base from the chromatograms.

High-temperature calorimetry. High-temperature microcalorimetry of NH_3 on zeolite catalyst was performed with a calorimeter (HAC-450G, Tokyo Rikou). The sample (1.5 g) was charged into the calorimeter and evacuated at 673 K for 4 h. NH_3 (15 mmol g^{-1}) was admitted to the cell dose after dose at 473 K.

Adsorption measurements. The adsorption uptake of methylamines was measured under vacuum with use of a McBain-type quartz spiral spring that was equipped with a displacement meter (Type 2U, Shinko Electronic), which was hung down to the sample basket. The catalyst was evacuated for 2 h at 773 K. After evacuation, 0.7 kPa of base molecules (MMA, DMA, TMA) were admitted at 373 K for several hours until adsorption had equilibrated. The

adsorption uptake of the methylamines were determined by the change in length of the spring.

IR spectroscopy. A vacuum-tight IR cell with KBr windows was designed to fit an infrared spectrometer (Hitachi 270-30) and to be attached to a vacuum system (10^{-4} Pa). The calcined portions of the zeolites were pressed into platelets with a thickness of about 10 mg cm^{-2}. These were mounted on a quartz rack that positioned then between the KBr windows (optical path length: 5 mm) of a vacuum-tight IR cell. The cell was arranged such that the zeolite wafer could be lowered into slots between the optical windows and withdrawn upward with use of a magnet into the heated portion for the pretreatment and adsorption of methylamines, NH_3 and methanol. After evacuation at 773 K for 1 h, the zeolite sample was cooled to 423 K before adsorption of the base molecules to be studied. Finally, the zeolite sample and its rack assembly were moved back between the KBr windows for recording of the spectroscopic data at room temperature.

XRF. The bulk ratio (Si/Al) was determined with use of XRF (Shimadzu XSF-1200); X-ray source, 40 kV, 70 mA, Rh target, with a FRC detector.

XRD. Powder patterns of the catalyst samples (placed on a glass plate) were recorded on a Rigaku Denki XRD (RAD-2A). The source was Cu$K\alpha$ (Ni filter).

MASNMR spectroscopy. The atomic ratio (Si/Al) and the chemical environment of Si and Al in the zeolite samples were determined by MASNMR. The zeolite samples were hydrated in a desiccator with saturated aqueous solution of NH_4Cl at room temperature for 24 h in order to minimize the linewidth of ^{27}Al. The MASNMR spectra were recorded at 53.7 and 70.4 MHz (referenced to TMS and $Al(H_2O)_6^{3+}$), for ^{29}Si and ^{27}Al, respectively, on a pulsed FT-NMR spectrometer (JNM-GX270, JEOL), which was equipped with a CP/MAS unit (NM-GSH27MU JEOL). All NMR spectra combined with magic angle spinning (MAS) spectra were recorded with H-decoupling during data acquisition. Cross-polarization (CP) was not employed, since the protons of zeolite samples are not directly attached to ^{29}Si or ^{27}Al. Each spectrum was recorded with 8 K data points and consisted of 700 to 1300 accumulated scans.

RESULTS AND DISCUSSION

Catalytic activity and selectivity for methylamine synthesis. The zeolite catalysts (acid-type) tested in this work include Y-type of faujasite (H-FAU), mordenite (H-MOR), ZSM-5 (H-MFI), ferrierite (H-FER), and chabazite (H-CHA). γ-Al_2O_3 and amorphous SiO_2–Al_2O_3 were also tested and used as references.

The catalyst performances under identical conditions are given in Table 1. Although γ-Al_2O_3 and amorphous SiO_2–Al_2O_3 give high methanol conversions, the selectivities for DME (31 and 58%) and TMA (12 and 31%) are rather high. The other zeolite catalysts in this study, H-FAU, H-MOR, and H-MFI show high activity for methanol amination, but the TMA selectivities (34–66%) are very high—close to the thermal equilibrium composition. Despite lower activity than others, H-FER catalyst still exhibits high selectivity for TMA (18%). Note that H-FER has a smaller pore size (0.42×0.54 nm) than the kinetic diameter of TMA (0.50 nm) (20). This suggests that TMA is formed on the *outer surface* catalytic sites. Only on H-CHA or on H-SC-MOR ($SiCl_4$-treated mordenite) is the selectivity for MMA and DMA higher than on the other catalysts. Moreover, H-CHA exhibits higher catalytic activity than H-SC-MOR; and no serious deactivation has been observed throughout the range of reaction conditions. We checked the XRD powder patterns of K-CHA and H-CHA at various ion-exchange levels to make sure that the crystal structures were correctly assigned. Comparison with published data (23) revealed the correct chabazite structure, except for

TABLE 1

Catalytic Activities and Selectivities for Methylamine Synthesis on Various Zeolite Catalysts

Catalyst	Si/Al	Pore size[a] (nm)	Methanol conversion (%)	Selectivity (yield) (%)			
				DME	MMA	DMA	TMA
γ-Al_2O_3			86	58 (50)	18 (15)	12 (10)	12 (10)
H-CHA	2.4	0.38×0.38	89	1 (1)	46 (41)	49 (44)	4 (4)
H-FAU	2.8	0.74×0.74	86	17 (15)	11 (9)	10 (9)	62 (53)
SiO_2–Al_2O_3	5.3		69	31 (21)	23 (16)	15 (10)	31 (21)
H-SC-MOR	7.5		52	7 (4)	48 (25)	41 (21)	3 (2)
H-FER	8.4	0.42×0.54	39	6 (2)	41 (16)	35 (14)	18 (7)
H-MOR	10.0	0.65×0.70	68	7 (5)	36 (24)	23 (16)	34 (23)
H-MFI	12.5	0.53×0.56	80	2 (2)	12 (10)	20 (16)	66 (53)

Note. Reaction temperature, 613 K; NH_3/CH_3OH, 2.0; *W/F*, 67 g h mol^{-1}; P_{MeOH}, 2.8 kPa.

[a] See Ref. 17.

TABLE 2

Methylamine Synthesis over H-CHA as a Function of Potassium Ion-Exchange Level

	Exchange level (%)	Acid amount[a] (mmol g^{-1})	Conversion (%)	Selectivity (%)			
				DME	MMA	DMA	TMA
K-CHA	—	0.03	28	10	34	25	31
H-CHA	44	0.20	60	5	46	32	17
H-CHA	76	0.49	89	1	46	49	4
H-CHA	89	1.09	96	—	48	49	3

Note. Reaction temperature, 613 K; NH_3/CH_3OH, 2.0; *W/F*, 67 g h mol^{-1}; P_{MeOH}, 2.8 kPa.
[a] Acid amounts was determined by microcalorimetry (>80 kJ mol^{-1}).

slight changes in relative intensities after ion-exchange from potassium to hydrogen from at various exchange levels. No crystal phase changes were observed before or after methanol amination reactions.

The catalytic activity of the H-CHA catalysts was evaluated as a function of extent of ion-exchange level (K^+-form to H^+-form). The results are shown in Table 2. Note that the K-CHA exhibits catalytic activity, albeit low (28%), while the selectivities for DME and TMA are both high. Potassium ion appears to catalyze TMA formation; since TMA is very bulky, catalytic reactions by K must be outside the cages. The analogous catalysis by sodium zeolites is well documented (13). As the H content is increased, activity increases also. However, more importantly, the selectivities for MMA and DMA are quite high, while only very small amounts of DME and TMA are obtained. The low yields of DME and TMA imply that their transition states are quite bulky and cannot be accommodated by the very small chabazite cages.

Vedrine *et al.* employed microcalorimetry at 423 K to characterize NH_3 adsorption on acid sites in H-MFI and found the stronger-acid site distribution more homogeneous in H-MFI than in H-FAU (21). We also used microcalorimetry (but at 473 K) to see only chemisorbed, and not physisorbed, NH_3 on the stronger-acid sites in H-CHA. The results, as a function of varying exchange level, are summarized in Fig. 1. All microcalorimetric curves decreased with increasing coverage of NH_3. At a higher ion exchange level (89%), H-CHA showed higher initial heat of adsorption (ca. 120 kJ mol^{-1}) than K-CHA (ca. 80 kJ mol^{-1}). Since a direct 1 : 1 relationship exists between the aluminum content of the framework and the number of positive charges due to the labile or exchangeable cations (22), this result shows that H-CHA catalysts at the 76–89% ion-exchange level have larger numbers of stronger-acid sites than K-CHA.

We employed high-resolution solid-state magic angle spinning NMR (MASNMR) to understand the structural features of the chabazites that gave very good activities and selectivities. For the potassium form (K-CHA) the relevant spectra are Figs. 2A and 2E; those for the hydrogen form (H-CHA) at varying ion-exchange levels are given in Figs. 2B and 2F, 2C and 2G, and 2D and 2H. In an aluminosilicate framework, there are five possibilities, described by the formula Si(nAl), where $n = 0$, 1, 2, 3, or 4. These five basic units of Si(nA1) mean that each silicon atom is linked, via oxygen, to n aluminum neighbors (24). The ^{29}Si-MASNMR spectra of K-CHA and H-CHA (Figs. 2A– 2D) show four different resonance peaks, which represent four kinds of Si-tetrahedra attached to different numbers of adjacent Al-tetrahedra: Si(3Al), Si(2Al), Si(1Al), and Si(0Al). The distribution as well as the relative intensities of Si(nAl) peaks in K-CHA (Fig. 2A) are different from those in H-CHA (Figs. 2B– 2D). Moreover, the relative intensities of Si(3Al) and Si(2Al) are decreased by increasing ion-exchange level (Si/Al ratios by NMR are given in the caption to Fig. 2). Therefore, some aluminum sites are removed from the chabazite framework during ion exchange.

The ^{27}Al-MASNMR spectra of chabazites (K-CHA and H-CHA) give one major sharp resonance peak at

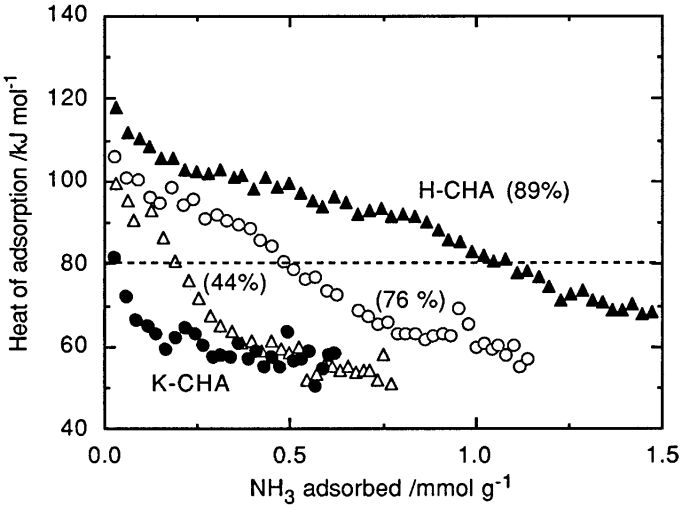

FIG. 1. High-temperature microcalorimetry of NH_3 on H-CHA at various ion exchange levels. NH_3 was adsorbed at 473 K.

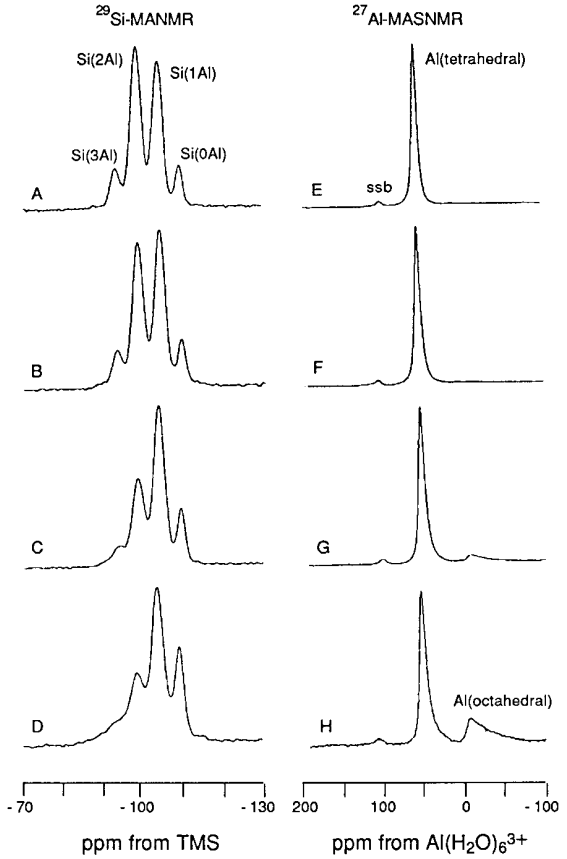

FIG. 2. ^{29}Si- and ^{27}Al-MASNMR spectra of chabazites before or after ion-exchange treatments from potassium to hydrogen form: (A, E) K-CHA (Si/Al = 2.5); (B, F) H-CHA (Si/Al = 2.7, 44%); (C, G) H-CHA (Si/Al = 3.1, 76%); (D, H) H-CHA (Si/Al = 3.4, 89%).

59 ppm (referenced to $Al(H_2O)_6^{+3}$). This is ascribed to the tetrahedral framework sites occupied by aluminum. At higher exchange level, another peak (−1.4 ppm, octahedral Al) builds up at the expense of the tetrahedral Al. K-CHA itself shows no detectable octahedral Al. If Al-octahedral can be minimized, then perhaps a H-CHA catalyst more active and selective than other zeolites can be obtained. Up to 76% ion-exchange level (Figs. 2C and 2G), H-CHA shows no detectable octahedral Al.

The catalytic performance of H-CHA (76%) is shown in Fig. 3. The activity rises with increasing partial pressures of NH_3. Importantly, TMA selectivity is extremely low (3–4%) and decreases slightly with higher partial pressures of NH_3, whereas MMA is the major product. The formation of DME and TMA is almost negligible up to about 90% methanol conversion. The conversion levels obtainable from H-CHA (76%) are higher than any of the other zeolite catalysts. Evidently, the smaller pore size (than other zeolites), which are 0.38×0.38 nm (see Table 1), and the inertness of external surfaces are the main causes for these activities and selectivities. If there are some active sites that are located on the external surfaces of H-CHA, the formation of TMA must be favorable.

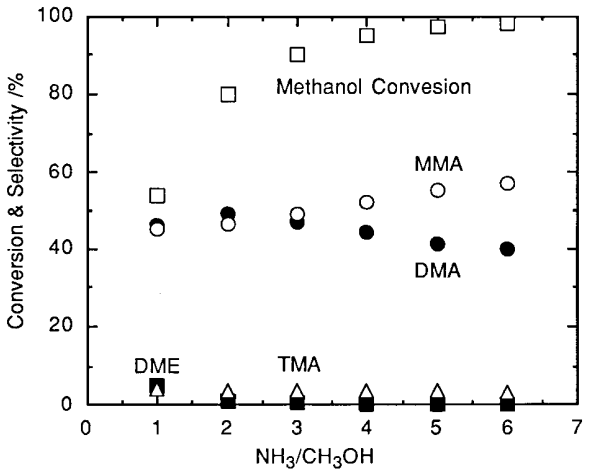

FIG. 3. Catalytic activities and selectivities for methylamine synthesis on H-CHA (Si/Al = 3.1, ion-exchange level = 76%) as a function of NH_3/CH_3OH: Reaction temperature = 613 K, $W/F = 67$ g h mol^{-1}, $P_{MeOH} =$ 2.8? kPa.

By contrast, methylamine synthesis over H-MOR (Si/Al = 10.0) is shown in Fig. 4. At lower partial pressures of NH_3, TMA is the major product, while the amount of DME is substantial. However, even when DME is diminished at higher pressures of NH_3, TMA selectivity remains quite high. Conversion levels (about 80%) are also lower than H-CHA.

We determined the effect of reaction temperature on the catalytic activity, conversion level, and selectivity of methanol amination over H-CHA catalysts (Si/Al, 2.2; ion-exchange level, 76%). The results (in Fig. 5) show those methanol conversion levels; TMA selectivity increased with

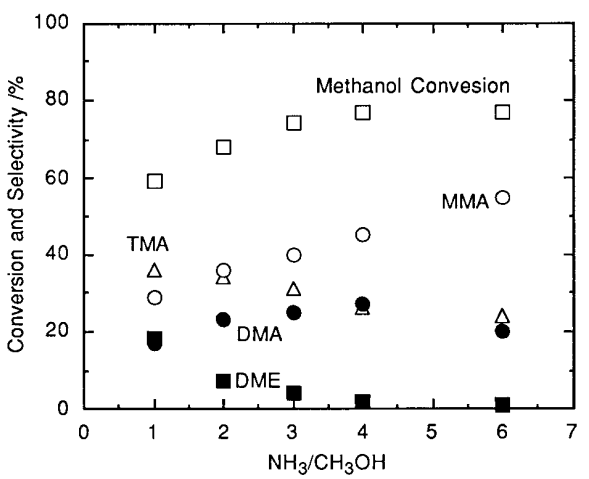

FIG. 4. Catalytic activities and selectivities for methylamine synthesis on H-MOR (Si/Al = 10.0) as a function of NH_3/CH_3OH: Reaction temperature = 613 K, $W/F = 67$ g h mol^{-1}, $P_{MeOH} = 2.8$ kPa.

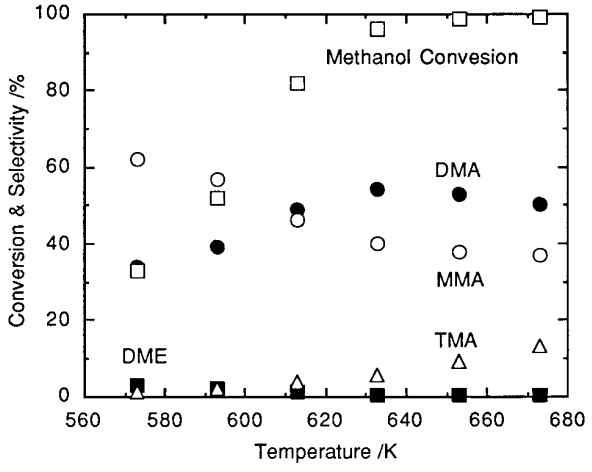

FIG. 5. Methylamine synthesis over H-CHA (Si/Al, 3.1; ion-exchange level, 76%) as a function of reaction temperature: $NH_3/CH_3OH = 2$, $W/F = 67$ g h mol^{-1}, $P_{MeOH} = 2.8$ kPa.

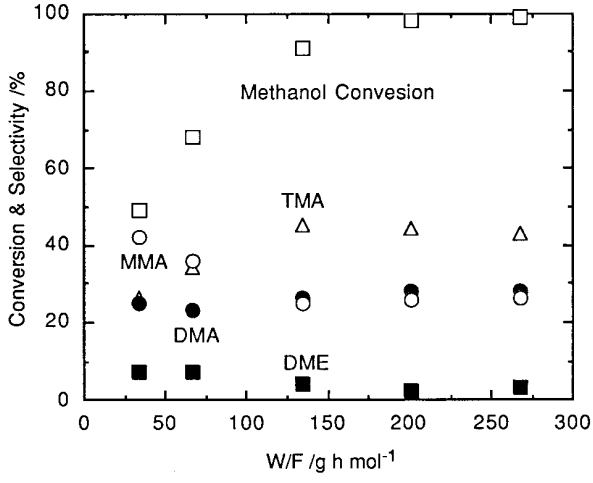

FIG. 7. Time courses of methylamine synthesis on H-MOR (Si/Al = 10.0) at 613 K: $W/F = 16.8$–100.5 g h mol^{-1}, $NH_3/CH_3OH = 2$, $P_{MeOH} = 2.8$ kPa.

increasing temperature. Importantly, however, below 620 K only neglibile amounts of TMA and DME were formed. These results suggest that H-CHA is a very selective catalyst for MMA and DMA.

The catalytic activity and selectivity for amination over H-CHA at 613 K as a function of contact time are shown in Fig. 6. MMA is the initial product, followed by DMA; however, TMA formation slightly increases with longer contact times. For instance, at long contact time ($W/F =$ 100.5 g h mol^{-1}) the product composition is MMA (43%), DMA (51%), and TMA (5%) at 95% methanol conversion ($NH_3/CH_3OH = 2$). This product composition is far from the thermal equilibrium values at 613 K: MMA (17%), DMA (24%), and TMA (59%). However, it is rather difficult to explain the TMA formation at high conversion region. Possibly, some mechanical defects in the catalyst framework, aggravated at elevated temperatures, unravel a few active sites on H-CHA; these can be fine tuned by future chemical treatment. If we compare the above time course with that of H-MOR (see Fig. 7), the product composition is very different. At longer contact time ($W/F = 268$ g h mol^{-1}), the methylamine compositions are MMA (26%), DMA (28%), and TMA (43%) at 99 % methanol conversion ($NH_3/CH_3OH = 2$).

Adsorption measurements and IR spectroscopy. We also measured the catalyst adsorption of methylamines with a vacuum balance. After evacuation at 773 K, the catalyst sample was exposed to 1.3 kPa of the amines at 373 K. Sorption uptake was monitored by the catalyst weight increase versus time. The result for H-MOR is shown in Fig. 8,

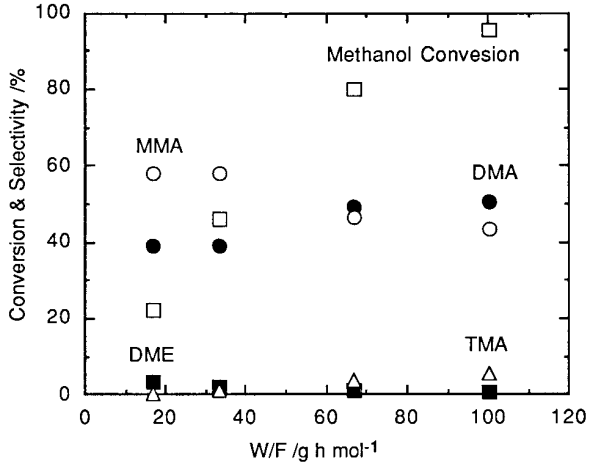

FIG. 6. Time courses of methylamine synthesis on H-CHA (Si/Al = 3.1, ion-exchange level = 76%) at 613 K: $W/F = 16.8$–100.5 g h mol^{-1}, $NH_3/CH_3OH = 2$, $P_{MeOH} = 2.8$ kPa.

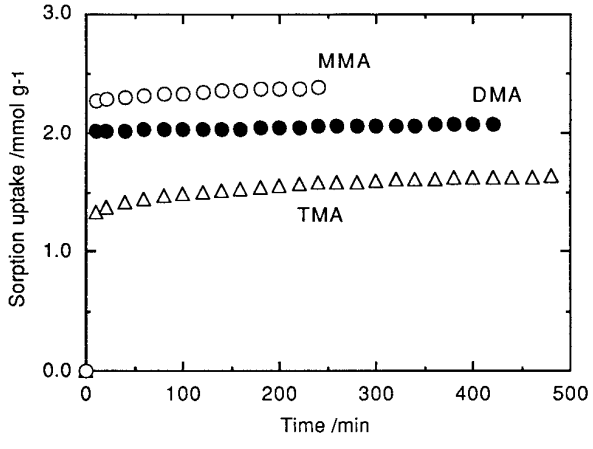

FIG. 8. Sorption profiles of methylamines over H-MOR (Si/Al = 9.7) as a function of exposure time at 373 K: $P_{MA} = 1.3$ kPa.

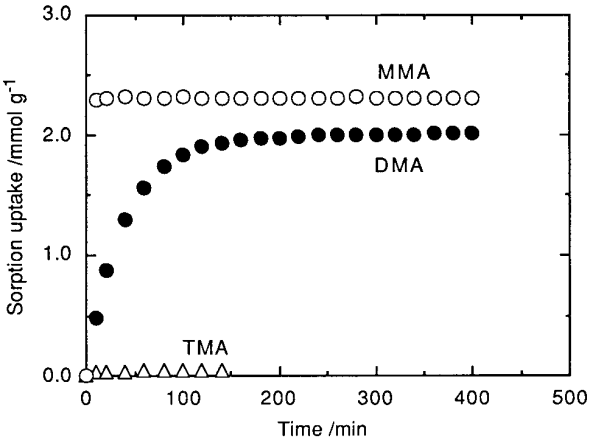

FIG. 9. Sorption profiles of methylamines over H-CHA (Si/Al = 3.1, ion-exchange level = 76%) as a function of exposure time at 373 K: P_{MA} = 1.3 kPa.

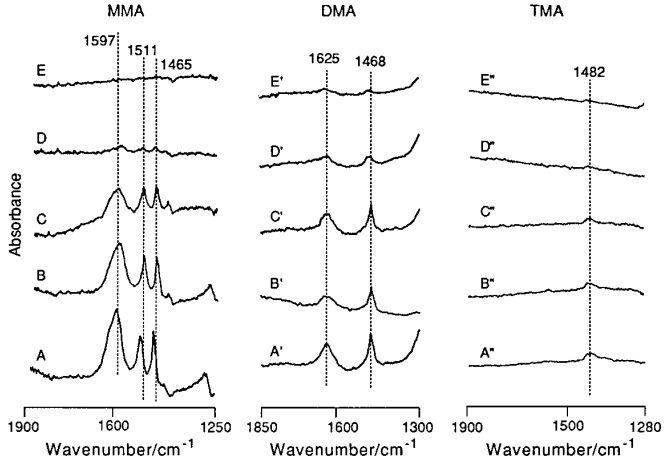

FIG. 10. IR spectra of adsorbed methylamines over H-CHA (Si/Al = 3.1, ion-exchange level = 7.6%): (A, A′ A″) adsorbed and evacuated at 333 K, (B, B′, B″) evacuated at 393 K, (C, C′, C″) evacuated at 473 K, (D, D′, D″) evacuated at 573 K, (E, E′ E″) evacuated at 693 K.

and that for H-CHA (76%) is shown in Fig. 9. H-MOR gets saturated quickly with MMA and DMA, whereas TMA requires a longer time to reach saturation. The sorption profiles on H-CHA are totally different. H-CHA gets saturated quickly by MMA, DMA takes a much longer saturation time, and TMA is almost completely excluded. The kinetic diameters of MMA, DMA, and TMA are 0.41, 0.44, and 0.50, respectively (20), while the pore sizes are 0.38×0.38 nm and 0.65×0.70 nm for H-CHA and H-MOR, respectively (see also Table 1). These sorption data correlate well with the higher selectivities for MMA and DMA on H-CHA than on H-MOR catalyst.

In order to learn more about the interactions of the different species (methanol, ammonia, MMA, DMA, and TMA) with the catalyst, we obtained a series of infrared spectra on H-MOR (Si/Al = 9.7) and H-CHA (Si/Al = 3.1, at 76% ion-exchange level). Methanol (at 0.5 kPa) or amines (at 0.3 kPa) were adsorbed on the catalyst for 0.5 h at 333 K and each spectrum was recorded upon evacuation at 333 K. Then the catalyst was heated under vacuum at 393, 473, and 673 K, and a spectrum was also taken at each temperature. The relevant portions of the IR spectra of MMA, DMA, and TMA on H-CHA at various temperatures are given in Fig. 10. The IR bands of pertinent species on both H-MOR and H-CHA are summarized in Table 3.

Adsorbed methanol on H-MOR exhibited bands (in cm^{-1}) at 3606 (ν OH, negative) and 3482 (ν OH, hydrogen bonded). At low temperatures, OH deformation bands were observed between 1900 and 1600, indicating intermolecular association; these bands disappeared from 393 K and above. The bands at 2960 (ν_{as} CH) and 2850 (ν_sCH) were observed along with 1468 (δ_{as} CH) and (δ_s CH) bands. These were completely gone at 673 K.

On H-CHA, methanol showed only four bands: 3660 (ν OH, negative), 2960 (ν_{as} CH), 2850 (ν_s CH), and 1466 (δ_{as} CH). The associated OH deformation bands and the symmetric CH deformation band were clearly absent. Methanol persisted on H-CHA up to 473 K but was completely desorbed at 673 K.

Adsorbed NH_3 on H-MOR showed a negative peak at 3606 (ν OH) and broad strong bands between 3250 and 2800; these bands disappeared almost completely at 673 K. The NH deformation band (intense, due to NH_4^+ species) was observed at 1443, but this was completely gone at 673 K. On H-CHA, the 3606 band and the 3200–200 bands were observed only up to 393 K. At lower temperatures the peaks at 1617 (δ_{as} NH, on Lewis acid site), 1450 (δ NH, as NH_4^+), and 1326 (δ_{as} NH, on Lewis acid site) (13) were observed up to 393 K, with bare traces at 473 K; they were completely gone above 573 K.

Adsorbed MMA on H-MOR persisted up to 573 K and showed the following: the 1609 peak (δ_{as} NH) maintained the same intensity from 333 to 573 K but with a slight upshift of ca. 10 cm^{-1} for every switch to the higher temperature. Evidently, MMA undergoes further reaction to DMA and TMA. At 673 K, the intensity of the 1609 peak dropped but that of the 1480 peak (δ_{as} CH of TMA) increased drastically. On H-CHA, MMA persisted up to 473 K (broad band at 3300–2800, ν NH); the band was completely gone at 573 K. The intensity of the asymmetric deformation band (δ_{as} NH) also broadened with decreased intensity but shifted slightly to a higher wavenumber upon heating (333 to 473 K). Remarkably, there was no detectable band near 1609–1613 (δ NH). Although this may suggest formation of TMA, as was the case with H-MOR, there was no detectable trace of a peak near 1480. This means lack of formation of TMA via subsequent reactions of MMA under these conditions.

The IR spectra of adsorbed DMA on H-MOR and H-CHA were also examined. On H-MOR, DMA showed

TABLE 3

Infrared Absorption Bands (in cm^{-1}) of Adsorbed Species on H-MOR and H-CHA Catalysts

Adsorbate	H-MOR		H-CHA	
CH_3OH	3606	ν OH (neg.)	3660	ν OH (neg.)
	3482	ν OH (H-bonded)	2960	ν_{as} CH
	2960	ν_{as} CH	2850	ν_s CH
	2850	ν_s CH	1466	δ_{as} CH
	1900–1600	δ OH (associated)		
	1468	δ_{as} CH		
	1390	δ_s CH		
NH_3	3606	ν OH (neg.)	3660	ν OH (neg.)
	3250–2800	ν NH	3200–2800	ν NH
	1443	δ_{as} NH (NH_4^+)	1617	δ_{as} NH (Lewis acid)
			1450	δ NH (NH_4^+)
			1326	δ_s NH (Lewis acid)
MMA	3606	ν OH (neg.)	3660	ν OH (neg.)
	3300–3000	ν NH	3200–2800	ν NH
	2969	ν_{as} CH	2958	ν_{as} CH
	2838	ν_s CH	2856	ν_s CH
	2750–2450	NH	1597	δ_{as} NH
	1609	δ_{as} NH	1511	δ_s NH
	1500	δ NH	1465	δ_{as} CH
	1462	δ_{as} CH	1424	δ_s CH
	1424	δ_s CH		
DMA	3606	ν OH (neg.)	3660	ν OH
	3250–3000	ν NH	3250–2800	ν NH
	2968	ν_{as} CH	2968	ν_{as} CH
	2802	ν_s CH	2804	ν_s CH
	2450	NH	1625	δ_{as} NH
	1613	δ_{as} NH	1468	δ_{as} CH
	1466	δ_{as} CH		
	1420	δ_s CH		
TMA	3606	ν OH (neg.)		
	3200–3000	ν NH		
	2962	ν_{as} CH		
	2748	ν_s CH		
	1480	δ_{as} CH	1482	δ_{as} CH

Note. The sample was adsorbed at 333 K for 0.5 h. The IR spectrum was recorded after evacuation at 333 K. The catalyst with adsorbed sample was heated under vacuum, and the spectrum recorded at 393, 473, 573, and 673 K. See text for explanation of results.

disproportionation to TMA as indicated by the shift of the 2802 peak (symmetric CH stretch of $N–CH_3$) to lower wavenumber (i.e., near 2762) from 333 up to 623 K. Likewise, the intensity of the 1480 peak of TMA increased at the expense of the 1466 peak of DMA. The intensity of NH deformation band, essentially unchanged up to 473 K, was significantly reduced at 623 K; this further confirmed the DMA reaction to TMA. Adsorbed DMA on H-CHA showed the expected bands (see Table 3) up to 473 K. The strongest bands at lower temperatures, namely 1625 and 1468, were but traces at 573 K and were completely gone at 673 K. The expected lack of TMA formation was confirmed.

Trimethylamine was also adsorbed on H-MOR and the characteristic bands persisted at all temperatures from 333 to 673 K (see Table 3). The 1480 peak (δ_{as} CH) became sharper and more intense at 673 K. Al lower temperatures, the symmetric CH stretch was broader than usual, and was slightly shifted to higher frequencies, suggesting disproportionation to lower alkylamines. On H-CHA, TMA was practically not adsorbed. Only a very slight trace of 1482 peak was detected, and this might represent outer surface species. At 573 K and higher, TMA was completely gone. These results suggest almost complete exclusion of TMA by H-CHA at the pertinent reaction temperatures (333–673 K) and confirm the very poor TMA uptake in the sorption experiments (see Fig. 9).

We also performed sequential adsorption of ammonia and methanol on the large pore zeolite (H-MOR) or on the small pore zeolite (H-CHA). The reaction was followed

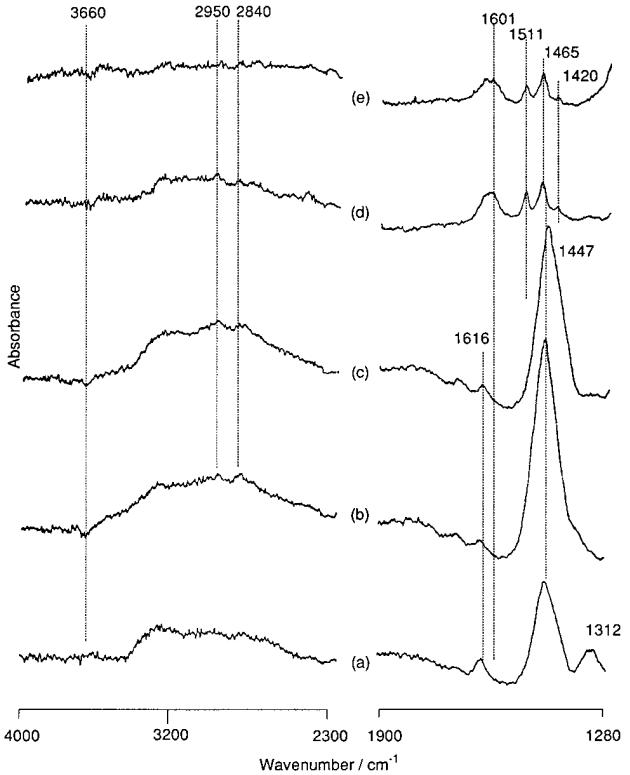

FIG. 11. IR spectra of adsorbed NH_3 and CH_3OH over H-CHA (Si/Al = 3.1, ion-exchange level = 76%): (a) NH_3 (1 kPa) was adsorbed on H-CHA at 333 K for 0.5 h and evacuated at 333 K. (b) After (a), CH_3OH was adsorbed next at 333 K for 0.5 h. (c) After (b), the catalyst sample was evacuated at 333 K. (d) After (c), the catalyst sample was heated, under no evacuation, at 5 K min^{-1} to 523 K. (e) After (d), catalyst sample was evacuated at 523 K.

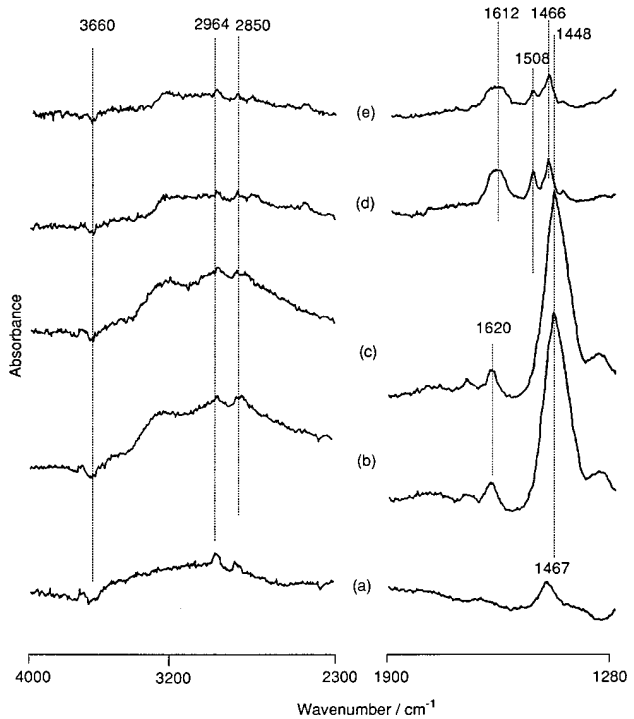

FIG. 12. IR spectra of adsorbed CH_3OH and NH_3 over H-CHA (Si/Al = 3.1, ion-exchange level = 76%): (a) CH_3OH (1 kPa) was adsorbed on H-CHA at 333 K for 0.5 h and evacuated at 333 K. (b) After (a), NH_3 was adsorbed next at 333 K for 0.5 h. (c) After (b), the catalyst sample was evacuated at 333 K. (d) After (c), the catalyst sample was heated, under no evacuation, at 5 K min^{-1} to 523 K. (e) After (d), catalyst sample was evacuated at 523 K.

by IR spectroscopy to understand the amination mechanism on the zeolite catalysts. On H-MOR, if methanol is adsorbed first, ammonia can displace the bound methanol and no methylamines are produced, even if the material is heated to 523 K. However, methylamines are obtained *only* if NH_3 is adsorbed first and heat is applied in the presence of free methanol. This is an Eley–Rideal mechanism (11, 13).

Although we have accumulated a great detail of IR spectroscopic data on H-MOR, we will not present them here because it gives higher TMA selectivity. Instead, because H-CHA afforded superior selectivity (low TMA fraction), we undertook a series of experiments to probe deeper into the reaction mechanism. Ammonia (1 kPa) was adsorbed on H-CHA for 0.5 h at 333 K followed by evacuation at 333 K. The IR spectrum (Fig. 11a) revealed Brønsted-site bound NH_3 (as NH_4^+, δ 1447, strong, broad) and Lewis-site bound NH_3 (δ 1616, weak). Methanol (1 kPa) was adsorbed next for 0.5 h at 333 K and the spectrum (Fig. 11b) showed a much larger peak near 1447. Evidently, submerged in this NH_4^+ peak were those of CH deformations (δ_{as} at 1468 and δ_s at 1390). The small peak near 1616 became even smaller. Upon evacuation at 333 K, the 1447 peak decreases slightly in intensity (Fig. 11c) but is still much larger than in Fig. 11a. This indicates that methanol and ammonia are both bound in the catalytic site, and, if such is the case, heating from 333 to 523 K at 5 K min^{-1} should give the alkylamine. The expected MMA was thus detected (see Figs. 11d and 11e) with its IR absorptions at 1601, 1511, 1465, and 1420, which represent δ_{as} NH, δ_s NH, δ_{as} CH, and δ_s CH, respectively.

We *reversed* the sequence of adsorption by allowing H-CHA to take up methanol first under conditions identical to those above. The IR spectrum (Fig. 12a) revealed bound methanol with peaks at 2964, 2850, and 1467, which represent ν_{as} CH, ν_s CH, and δ_{as} CH, respectively. After adsorption of ammonia (1 kPa) for 0.5 h at 333 K, the spectrum (Fig. 12b) showed an intense peak centered at 1448 (δ NH_4^+) and a weaker peak near 1620 (δ_{as} NH on Lewis site). The catalyst sample was evacuated at 333 K and the spectrum revealed practically unchanged NH deformation bands. If methanol had been displaced by ammonia, the size of the 1448 band would make it undetectable, particularly after evacuation. If so, heating would give no alkylamines (as was the case with H-MOR). However, the spectrum

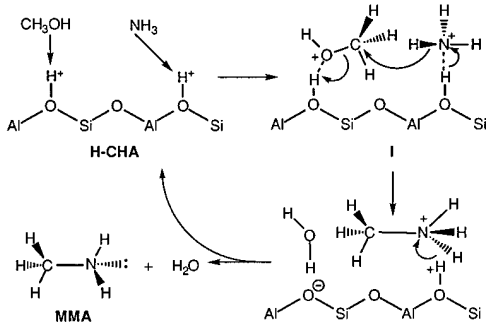

SCHEME I. Proposed mechanism for methylamine synthesis. Methanol and ammonia are adsorbed on adjacent Brønsted acid sites to give proximally bound species (I). An analogous "intramolecular" SN_2 reaction between bound species produces water and protonated amine. Proton transfer to oxygen regenerates the catalyst. Limited space in H-CHA cages precludes formation of bulky transition states; hence the term "transition state selectivity."

(Figs. 12d and 12e) obtained after heating 333 to 523 K at 5 K min^{-1} revealed the presence of MMA: 2964 (ν_{as} CH), 2850 (ν_s CH), 1612 (δ_{as} NH), 1508 (δ_s NH), 1466 (δ_{as} CH), and 1424 (δ_s CH). These results suggest that heating at 523 K consummates the reaction over H-CHA between methanol and ammonia that are *both* bound to the catalytic site. This explains why the order of introduction of reagents is immaterial. This reaction of both catalytically bound methanol and ammonia via small pore zeolite (H-chabazite) fits into the Langmuir–Hinshelwood mechanism and differs mechanistically from the H-MOR catalyzed reaction (Eley–Rideal mechanism). The proposed reaction mechanism is shown in Scheme I.

Because H-CHA has only a very small number of external catalytic sites (if any), the reaction between two proximally *bound* species inside the cage disfavors the formation of bulky products such as TMA. Even if TMA should form inside (unlikely for H-CHA), it cannot escape through the pores and mix with the product stream. Thus, the product mixture is rich in MMA and DMA. Interestingly, the yield of DME is also very low, even if its size approximates that of DMA. However, DME is formed via Eley–Rideal mechanism: two methanols react; one is unbound, the other is bound to a Brønsted acid site (11, 14). Such a transition state is sterically demanding. Therefore, the traces of DME must be formed externally on sites that impose no restrictions on the sizes of transition states.

CONCLUSION

The reaction between methanol and ammonia was studied on various zeolite catalysts. The results showed that H-CHA catalyzes the reaction with higher selectivity than others. The selectivity for MMA plus DMA was about 97% at 98% methanol conversion ($NH_3/CH_3OH = 6.0$, 613 K). Brønsted acid sites along the chabazite cages (correct crystal structure obtained by XRD powder patterns) provide the catalytic activity for methylamine synthesis. Only very small amounts of DME and TMA are formed; this is explainable in terms of residual active sites outside the framework. The IR spectral data of adsorbed species and the methylamine sorption uptake prove that TMA cannot penetrate the narrow chabazite cages, which are accessible only to the reactants or MMA and DMA. IR data also suggest that initial MMA formation occurs between two proximally bound species; otherwise, the reaction cannot transpire because of space restrictions. This effectively excludes formation of TMA in the cage, which requires a very bulky transition state. Even if a trace of TMA can form inside the cage, it cannot diffuse out because of its bulk, and its only alternative is thermal disproportionation to lower alkylamines. Even DME formation, believed to occur via Eley–Rideal mechanism, is very low on H-CHA. DME formation requires weakly acidic sites, which reside mainly on the external surfaces of zeolites. However, the external surfaces of H-CHA are nearly inert already. Therefore, low DME selectivity in chabazites is another manifestation of transition state selectivity. In many respects, H-CHA catalyst displays better shape selectivity for lower alkylamines in methanol amination. We have presented evidence in support of the Langmuir–Hinshelwood mechanism in H-CHA catalysis of methylamine synthesis.

REFERENCES

1. Weissermel, K., and Arpe, H. J., "Industrial Organic Chemistry," p. 45. Verlag Chemie, New York, 1978.
2. Ashina, Y., Fujita, T., Fukatsu, M., and Yagi, J., Eur. patent appl. 130,407 (1984).
3. Weigert, F. J., *J. Catal.* **103**, 20 (1987).
4. Keane, Jr., M., Sonnichsen, G. C., Abrams, L., Corbin, D. R., Gier, T. E., and Shannon, R. D., *Appl. Catal.* **32**, 361 (1987).
5. Abrams, L., Shannon, R. D., and Sonnichsen, G. C., U.S. patent 4,737,592 (1988); Abrams, L., Keane, Jr., M., and Sonnichsen, G. C., *J. Catal.* **115**, 410 (1989).
6. Gier, T. E., Shannon, R. D., Corbin, D. R., and Keane, Jr., M., U.S. patent 4,806,689 (1989); U.S. patent 4,602,112 (1986).
7. Shannon, R. D., Keane, Jr., M., Abrams, L., Staley, R. H., Gier, T. E., Corbin, D. R., and Sonnichsen, G. C., *J. Catal.* **113**, 367 (1988).
8. Shannon, R. D., Keane, Jr., M., Abrams, L., Staley, R. H., Gier, T. E., Corbin, D. R., and Sonnichsen, G. C., *J. Catal.* **114**, 8 (1988).
9. "Ullmanns Encyclopädie der Technischen Chemie," 4th ed., Vol. 17, p. 9; Vol. 16, p. 671. Verlag Chemie, Weinheim, 1978.
10. Ramioulle, J., and David, A., *Hydrocarbon Process.* **7**, 113 (1981).
11. Mochida, I., Yasutake, I., Fujitsu, H., and Takeshita, K., *J. Catal.* **82**, 313 (1993).
12. Dingerdissen, U., "Herstellung von niederen Aminen an Zeolithkatalysatoren," VDI-Fortschrittsber 219. VDI-Verlag, Düsseldorf, 1990.
13. Kogelbauer, A., and Lercher, J. A., *J. Chem. Soc. Faraday Trans.* **88**, 2283 (1992).
14. Fetting, F., and Dingerdissen, U., *Chem. Eng. Technol.* **15**, 202 (1992).
15. Shannon, R. D., Keane, Jr., M., Abrams, L., Staley, R. H., Gier, T. E., Corbin, D. R., and Sonnichsen, G. C., *J. Catal.* **115**, 79 (1988).

16. Bergna, H. E., Keane, Jr., M., Ralston, D. H., Sonnichsen, G. C., Abrams, L., and Shannon, R. D., *J. Catal.* **115**, 148 (1988).
17. Corbin, D. R., Keane, M., Jr., Abrams, L., Farlee, R. D., Bierstedt, P. E., and Bein, T., *J. Catal.* **124**, 268 (1990).
18. Nasikin, M., Nakamura, R., and Niiyama, H., *Chem. Lett.* 202 (1993).
19. Segawa, K., and Tachibana, H., *J. Catal.* **131**, 482 (1991).
20. Foley, H. C., Lafyatis, D. S., Mariwala, R. K., Sonnichsen, G. D., and Brake, L. D., *Chem. Eng. Sci.* **49**, 4771 (1994).
21. Vedrine, J., Auroux, A., Dejave, P., Ducatme, V., Hoser, H., and Zhou, S., *J. Catal.* **73**, 147 (1982).
22. Derouane, E. G., *in* "Intercalation Chemistry" (M. S. Whittingham and A. J. Jacobson, Eds.), p. 101. Academic Press, New York, 1982.
23. Ballmoos, R. V., and Higgins, J. B., "Collection of Simulated XRD Powder Patterns for Zeolites," 2nd ed., p. 368S. Butterworth-Heinemann, Stoneham, MA, 1990.
24. Thomas, J. M., and Klinowski, J., *Adv. Catal.* **33**, 199 (1985).